

Microscopic structure of oxygen defects in gallium arsenide

M. Pesola

Laboratory of Physics, Helsinki University of Technology, P.O. Box 1100, FIN-02015 HUT, Finland

J. von Boehm

LTAM, Helsinki University of Technology, P.O. Box 1100, FIN-02015 HUT, Finland

V. Sammalkorpi

Laboratory of Physics, Helsinki University of Technology, P.O. Box 1100, FIN-02015 HUT, Finland

T. Mattila

*Laboratory of Physics, Helsinki University of Technology, P.O. Box 1100, FIN-02015 HUT, Finland
and National Renewable Energy Laboratory, Golden, Colorado 80401*

R. M. Nieminen

Laboratory of Physics, Helsinki University of Technology, P.O. Box 1100, FIN-02015 HUT, Finland

(Received 30 April 1999; revised manuscript received 11 October 1999)

Accurate total-energy pseudopotential methods are used to study the structures, binding energies, and local vibrational modes of various models for the Ga-O-Ga defect in GaAs. We find that the previously proposed models, O_{As} (an off-centered substitutional oxygen in arsenic vacancy) and O_I (an oxygen atom occupying a tetrahedral interstitial site), are inconsistent with experimental data. We introduce a model, $(As_{Ga})_2-O_{As}$ (two arsenic antisites and one off-centered substitutional oxygen in arsenic vacancy), the properties of which are in excellent agreement with experimental characterizations. [S0163-1829(99)51648-2]

Oxygen is the most important unintentional impurity in GaAs—a situation resembling that in Si. The as-grown GaAs crystal is semi-insulating and As-rich, containing about 10^{16} EL2 defects/cm³, identified as As_{Ga} antisites.^{1,2} Oxygen in the puckered bond-center defect Ga-O-As gives rise to an experimentally detected local vibration (LV) frequency doublet at 845 cm^{-1} .² In addition, LV frequencies are detected also at 731 and 715 cm^{-1} (*A* and *B*, respectively).³ These frequencies show the characteristic triplet fine structures caused by the ⁶⁹Ga and ⁷¹Ga isotopes,^{3,4} and the ¹⁸O→¹⁶O isotopic shifts² leading to the unambiguous conclusion that the frequencies originate from a Ga-O-Ga structure. We call the defect containing this Ga-O-Ga structure simply the Ga-O-Ga defect. The as-grown GaAs crystal contains about 10^{15} Ga-O-Ga defects/cm³.^{5,6} The LV modes show photosensitivity: in semi-insulating GaAs, band *A* can be converted by illumination into band *B* via a third band *B'* located 0.7 cm^{-1} below *B*.^{3,6,7} *A*, *B'*, and *B* are zero-, one-, and two-electron states of the Ga-O-Ga defect, respectively.⁶ The Ga-O-Ga defect shows a negative-*U* property,⁶ *B'* being a metastable paramagnetic state.⁸

Conventionally, the Ga-O-Ga defect has been thought to consist of an arsenic vacancy (V_{As}) and a substitutional O atom having a tendency to get displaced from the vacancy site in the [001] direction in negative charge states. This O_{As} model—used almost exclusively in interpreting experimental data—is thus very similar to the *A* center in silicon (an off-centered substitutional O atom in a vacancy, denoted by $V_{Si}O$ in this paper).⁹ The density-functional-theoretic (DFT) cluster calculations in the local density approximation (LDA) (Ref. 10) for GaAs by Jones and Öberg¹¹ give, consistently

with the experiments, a significant decrease in the LV frequency when O_{As} is charged with two electrons. However, according to the more recent DFT LDA supercell calculations by Mattila and Nieminen,¹² and Taguchi and Kageshima,¹³ the distance of the O atom from the off-centered substitutional arsenic site *increases* with increasing electronic charge analogously to $V_{Si}O$.¹⁴ For this defect, the LV frequency of the asymmetric stretching mode *increases*¹⁴ which indicates a similar behavior for O_{As} in disagreement with the experimental change from *A* to *B*.

Taguchi and Kageshima¹³ also criticized the O_{As} model of having too weak a negative-*U* character, and proposed instead a model where the O atom occupies a tetrahedral interstitial (T_d) site at negative charge states, but moves towards the neighboring As atom along the [001] direction in the neutral state, coupling with two Ga atoms (called here the O_I model, not to be mixed with the Ga-O-As defect). This model indeed has a stronger negative-*U* property than the O_{As} model¹³ but turns out to be less successful in describing the LV's.

In this Rapid Communication, we show by using accurate total-energy DFT LDA pseudopotential (PP) methods,¹⁵ that the two previously proposed models, for the Ga-O-Ga defect (O_{As} and O_I) are inconsistent with the experiments, and introduce a model that is shown to be in agreement with the experiments. This model is presented schematically in Fig. 1 and consists of two arsenic antisites (As_{Ga}) and one off-centered substitutional oxygen in arsenic vacancy [$(As_{Ga})_2-O_{As}$].

The DFT LDA total energy calculations are performed using a self-consistent plane-wave PP method.¹⁵ For oxygen

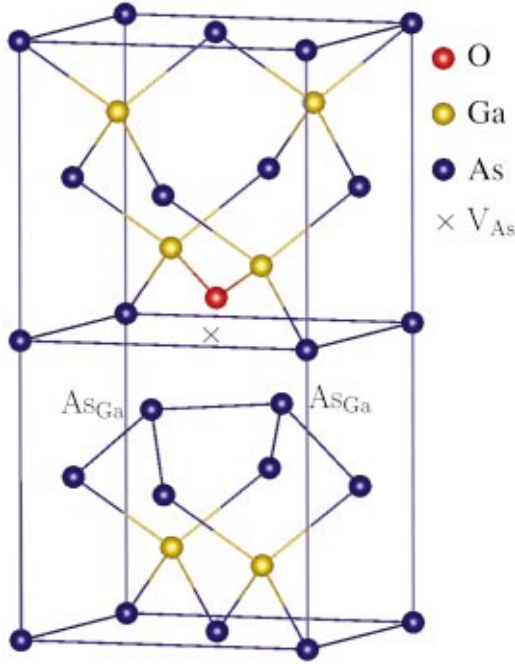


FIG. 1. Two conventional GaAs unit cells with the $(\text{As}_{\text{Ga}})_2\text{-O}_{\text{As}}$ defect (schematically). Yellow balls denote gallium and blue balls arsenic atoms. A red ball denotes the oxygen atom, and a cross the arsenic vacancy (V_{As}). The two arsenic antisites (As_{Ga}) are marked in the figure.

we use the ultrasoft Vanderbilt pseudopotential.¹⁶ For Ga and As, we use the normconserving Hamann PP,¹⁷ with the nonlinear core valence exchange-correlation scheme.¹⁸ The Ga and As $3d$ -electrons are included in the pseudocore. The effect of this approximation was studied by generating a PP for Ga, which includes $3d$ electrons in the valence. Though the bulk properties of the GaAs crystal were improved, the effect on the O-Ga interaction turned out to be marginal. The valence-electron wave functions are expanded in a plane-

wave basis set up to a kinetic-energy cutoff of 25 Ry. We use the Monkhorst-Pack 2^3 \mathbf{k} -point sampling¹⁹ and a 32 atom-site supercell in calculating the LV modes. To confirm the convergence of our results, a 128 atom-site supercell with the Γ point is also used in calculating structures. Unless otherwise stated, the calculated results are obtained with 2^3 \mathbf{k} points and a 32 atom-site supercell.²⁰ To find the equilibrium configurations, the total energy is minimized by allowing all ionic coordinates to relax without any constraints. In calculating the formation energies for different charge states, Q , the valence band maxima E_V^Q are aligned using the average potential corrections.²¹ The LV calculations are performed in the relaxed minimum energy configuration using the procedure and program by Köhler *et al.*:²² Every atom is displaced to all six Cartesian directions from the equilibrium position, the electronic structures for these configurations are optimized, and the resulting Hellman-Feynman forces are calculated. The coupling constants for the dynamical matrix are calculated by finite differences using these forces and displacements. For a more detailed description of the methods, see Refs. 14,15.

Table I shows the calculated structures and LV frequencies for the three models O_{As} , O_{I} , and $(\text{As}_{\text{Ga}})_2\text{-O}_{\text{As}}$, as well as the experimental LV frequencies for the Ga-O-Ga defect.^{2,6} For reference, we note that our calculated value of 869 cm^{-1} for the asymmetric stretching LV frequency of the Ga-O-As defect agrees closely with the measured vibration frequency of 845 cm^{-1} ,² the difference being a signature of the tendency of LDA for overbinding.

First consider O_{As} . The calculated structure and the LV frequencies of O_{As} change analogously to $V_{\text{Si}}\text{O}$ in Si when the defect is charged.¹⁴ The occupation of the antibonding defect state shortens the Ga-O bonds, increases the Ga-O-Ga angle and the Ga-Ga bond length, leading to higher LV frequencies. The calculated changes in the structure induced by charging (Table I) are similar to those reported in Refs. 12,13. The effect of charging on the LV frequencies is *op-*

TABLE I. Calculated structures and vibrational frequencies for the defect models. LVF denotes local vibration frequency. For O_{As} and $(\text{As}_{\text{Ga}})_2\text{-O}_{\text{As}}$, only the uppermost (asymmetric) LVF is given, while for O_{I} all degenerate LVF's are listed. The calculated LVF's for the ^{16}O and ^{18}O isotopes are given in the fifth and sixth columns, respectively, and the corresponding experimental values in the final two columns (the values in parentheses give the isotopic shifts $^{16}\text{O}\rightarrow^{18}\text{O}$).

Defect Charge state	Bond length Ga-O (Å)	Ga-O-Ga angle (deg)	Bond length Ga-Ga (Å)	LVF ^{16}O (cm^{-1})	LVF ^{18}O (cm^{-1})	State	Expt. ^{16}O (cm^{-1})	Expt. ^{18}O (cm^{-1})
O_{As}			Ga-Ga					
-1	1.82	132	2.61	648	615(-33)			
-3	1.79	141	2.62	705	669(-36)			
O_{I}								
0	~ 1.9	~ 120		588,578				
-1	~ 2.0	~ 110		499,486,426				
-2	~ 2.0	~ 110		472,468,467				
$(\text{As}_{\text{Ga}})_2\text{-O}_{\text{As}}$			$(\text{As}_{\text{Ga}})\text{-(As}_{\text{Ga}})$					
+1	1.775	140.1	3.36	748	709(-39)	A	730.7 ^a	
0	1.780	138.7	2.98	734	697(-37)	B'	714.2 ^a	
-1	1.778	138.4	2.60	738	700(-38)	B	714.9 ^a	679 ^b (-36)

^aReference 6.

^bReference 2.

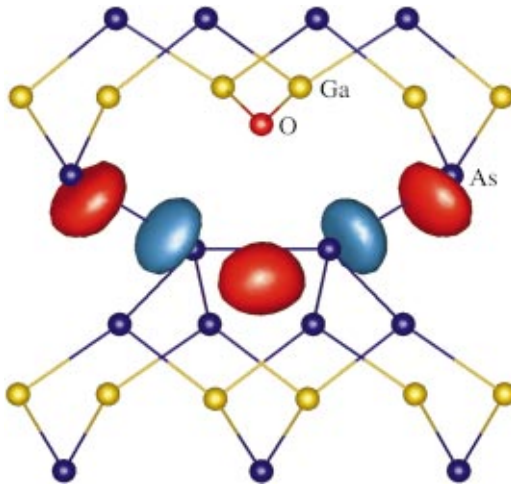


FIG. 2. A constant-value surface of the electron density of the uppermost occupied electronic state of the negative charge state of $(\text{As}_{\text{Ga}})_2\text{-O}_{\text{As}}$. The electron density isosurface is at half of the maximum value of $0.03e/\text{\AA}^3$. Yellow balls denote gallium, and blue balls arsenic atoms. A red ball denotes the oxygen atom. A red surface indicates positive wave function and a blue surface negative one.

posite to that observed in the infrared (IR) absorption measurements (Table I). Thus our calculations do *not* support the idea that O_{As} would be the experimentally observed Ga-O-Ga defect.

For the O_1 model by Taguchi and Kageshima,¹³ we find that in the neutral charge state the oxygen atom is practically threefold coordinated with similar bonds to three neighboring Ga atoms surrounding the T_d site. This leads to degeneracy and significantly lower LV frequencies compared to the experimental values (Table I). In the negative charge states, the oxygen atom is located very near the T_d site with four similar O-Ga bonds leading again to degeneracy, and significantly lower LV frequencies compared to the experimental values (Table I). In addition, we find that the calculated total energy of the O_1 model in the neutral charge state is 1.4 eV higher than that of the neutral Ga-O-As defect. Thus, our results also exclude the O_1 model from being a possible microscopic model for the Ga-O-Ga defect.

Consider then the $(\text{As}_{\text{Ga}})_2\text{-O}_{\text{As}}$ defect model. Figure 2 shows the calculated electron density of the uppermost electronic state occupied by two electrons in the singly negative charge state of $(\text{As}_{\text{Ga}})_2\text{-O}_{\text{As}}$ (obtained with a 128 atom-site supercell and the Γ point). The wave function is almost 10- \AA wide, which can explain the broad 90-mT half-width of the electronic paramagnetic resonance peak observed by Linde *et al.*⁸ The electronic wave function is clearly localized in the plane determined by the O atom and the two As_{Ga} 's (Figs. 1 and 2). The corresponding electron density has a distinct maximum between the As_{Ga} 's, and the wave function is of the *bonding* type, in contrast to the antibonding state appearing in O_{As} or $\text{V}_{\text{Si}}\text{O}$.^{9,14} However, the wave function is antibonding between the subsequent $\text{As}_{\text{Ga}}\text{-As}$ pairs (Fig. 2) which further stresses the bonding nature between the As_{Ga} 's. The bonding nature of the electronic wave function is clearly seen in the $\text{As}_{\text{Ga}}\text{-As}_{\text{Ga}}$ distance, which *shortens* by 0.76 \AA when two electrons are added (Table I). This behavior is *opposite* to the antibonding behavior of the Si-Si

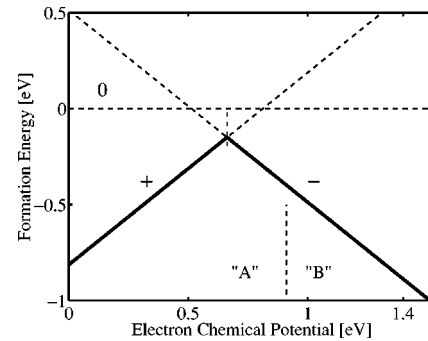


FIG. 3. Formation energy plot for the $(\text{As}_{\text{Ga}})_2\text{-O}_{\text{As}}$ defect. The thick line indicates the charge state with the lowest energy. The energy of the metastable neutral charge state is taken as the reference energy. The experimental band-gap value of 1.53 eV is used to give the upper limit for the electron chemical potential. "A" and "B" denote the two experimentally observed (Refs. 3 and 6) stable states separated by an ionization level.

and Ga-Ga bonds of $\text{V}_{\text{Si}}\text{O}$ (Ref. 14) and O_{As} (Table I), respectively. Accordingly, the charge-state induced shifts in the LV frequencies of $(\text{As}_{\text{Ga}})_2\text{-O}_{\text{As}}$ should be opposite to those of O_{As} . This is exactly what we find. The calculated LV frequencies for $(\text{As}_{\text{Ga}})_2\text{-O}_{\text{As}}$ show a *clear downwards shift* in agreement with the experiments (Table I). The calculated frequency shifts from A to B' and from B' to B are -13 and 3 cm^{-1} , in close agreement with the corresponding experimental values of -16.5 and 0.7 cm^{-1} . Thus the experimental observation that the LV frequency of B' is lowest is also seen in our calculations.

Changing the oxygen isotope ^{16}O into ^{18}O we obtain a frequency of 701 cm^{-1} for B in close agreement with the measured frequency of 679 cm^{-1} (Table I). The calculated isotopic shift of -38 cm^{-1} is in very close agreement with the experimental shift of -36 cm^{-1} (Table I).

Figure 3 shows the formation energy plot obtained from the total energy calculations for $(\text{As}_{\text{Ga}})_2\text{-O}_{\text{As}}$. It has a $(-/+)$ ionization level at about $E_v + 0.7 \text{ eV}$ (E_v denotes the valence band maximum) in the forbidden energy gap and exhibits a strong negative- U property, the neutral charge state being thermodynamically metastable. This is in close agreement with the experimental results by Alt who finds that the ionization level for the second electron is at $E_c - 0.65 \text{ eV}$ (E_c denotes the conduction band minimum).^{6,23}

Early studies by Watkins and Corbett showed that $\text{V}_{\text{Si}}\text{O}$ reorients with a barrier of 0.38 eV when uniaxial stress is applied to the Si crystal.⁹ However, Song *et al.*²⁴ concluded from their piezospectroscopic measurements that the Ga-O-Ga defect does *not* reorient in GaAs. Both O_{As} and O_1 have no structural reason that would hinder their reorientation. The presence of two As_{Ga} 's in the $(\text{As}_{\text{Ga}})_2\text{-O}_{\text{As}}$ model for the Ga-O-Ga defect explains the absence of reorientation in a natural way (see Fig. 1).

The deep-level transient spectroscopy experiments by Samara *et al.*²⁵ show that the distance ΔE from the defect level to E_c of the Ga-O-Ga defect, increases under applied pressure P by $8.4 \pm 1.0 \text{ meV/kbar}$. Estimating $\Delta E(P)$ by using one-electron eigenvalues,²⁶ we get for ΔE an increase of roughly 3 meV/kbar , in reasonable agreement with the experimental value above.

TABLE II. Calculated binding energies E_b for $(\text{As}_{\text{Ga}})_2\text{-O}_{\text{As}}$ and O_{As} .

Constituents	→	Outcome	E_b (eV)
$[\text{As}_{\text{Ga}}]^{2+} + [\text{V}_{\text{Ga}}]^{3-} + \text{O}_i$	→	$[(\text{As}_{\text{Ga}})_2\text{-O}_{\text{As}}]^-$	1.2
$[\text{As}_{\text{Ga}}]^{2+} + [\text{V}_{\text{Ga}}]^- + \text{O}_i$	→	$[(\text{As}_{\text{Ga}})_2\text{-O}_{\text{As}}]^+$	3.1
$[\text{V}_{\text{As}}]^- + \text{O}_i$	→	$[\text{O}_{\text{As}}]^-$	3.3
$2 \text{As}_{\text{Ga}} + [\text{O}_{\text{As}}]^-$	→	$[(\text{As}_{\text{Ga}})_2\text{-O}_{\text{As}}]^-$	2.7
$2 \text{As}_{\text{Ga}}^{2+} + [\text{O}_{\text{As}}]^{3-}$	→	$[(\text{As}_{\text{Ga}})_2\text{-O}_{\text{As}}]^+$	3.2

Due to the apparent complexity of $(\text{As}_{\text{Ga}})_2\text{-O}_{\text{As}}$, it is important to consider its formation processes and stability. Table II lists the calculated binding energies for $(\text{As}_{\text{Ga}})_2\text{-O}_{\text{As}}$ and O_{As} . $(\text{As}_{\text{Ga}})_2\text{-O}_{\text{As}}$ may be thought to consist of dissolved oxygen, As_{Ga} , and V_{Ga} , because V_{Ga} is metastable and has a tendency to form an $\text{As}_{\text{Ga}}\text{-V}_{\text{As}}$ complex.^{1,27,28} The resulting binding energy is rather large (3.1 eV) for the positive charge state of $(\text{As}_{\text{Ga}})_2\text{-O}_{\text{As}}$ and somewhat smaller (1.2 eV) for the negative one (first two rows in Table II). The binding energy of O_{As} in the negative charge state is 3.3 eV. However, O_{As} has a clear tendency to further bind with two As_{Ga} 's to form $(\text{As}_{\text{Ga}})_2\text{-O}_{\text{As}}$ [energy gain of 2.7 eV for the negative $(\text{As}_{\text{Ga}})_2\text{-O}_{\text{As}}$ and 3.2 eV for the positive

$(\text{As}_{\text{Ga}})_2\text{-O}_{\text{As}}$, last two rows in Table II] thus supporting our proposal for the Ga-O-Ga defect. To summarize, we find that there are (at least) two pathways of forming a stable $(\text{As}_{\text{Ga}})_2\text{-O}_{\text{As}}$ (first two and last two rows in Table II).

In conclusion, a microscopic $(\text{As}_{\text{Ga}})_2\text{-O}_{\text{As}}$ model for the Ga-O-Ga defect has been introduced. All properties of this defect model are consistent with the experimental findings. $(\text{As}_{\text{Ga}})_2\text{-O}_{\text{As}}$ exhibits negative- U behavior, the neutral charge state being thermodynamically metastable. The calculated shifts induced by charging as well as the isotopic shifts in the LV frequencies agree closely with the experimental ones. The downwards shift in the LV frequency $A \rightarrow B$, induced by charging, is shown to originate from the bonding nature of the defect state in the forbidden energy gap. The $(\text{As}_{\text{Ga}})_2\text{-O}_{\text{As}}$ model contains two As_{Ga} 's, and therefore the EL2 defect related closely to As_{Ga} may be an essential part of the Ga-O-Ga defect.

The authors wish to thank Dr. K. Saarinen, Dr. S. Pöykkö, Professor M. Puska, and Professor P. Hautojärvi for many valuable discussions. This work has been supported by the Academy of Finland. T.M. acknowledges the financial support of the Väisälä Foundation. M.P. acknowledges the financial support of the Väisälä Foundation and of the Finnish Cultural Foundation. We acknowledge the generous computing resources of the Center for the Scientific Computing (CSC), Espoo, Finland.

- ¹J.C. Bourgoin, H.J. von Bardeleben, and D. Stiévenard, *J. Appl. Phys.* **64**, R65 (1988).
- ²J. Schneider, B. Dischler, H. Seelewind, P.M. Mooney, J. Lagowski, M. Matsui, D.R. Beard, and R.C. Newman, *Appl. Phys. Lett.* **54**, 1442 (1989).
- ³C. Song, W. Ge, D. Jiang, and C. Hsu, *Appl. Phys. Lett.* **50**, 1666 (1987).
- ⁴X. Zhong, D. Jiang, W. Ge, and C. Song, *Appl. Phys. Lett.* **52**, 628 (1988).
- ⁵G.M. Martin and S. Makram-Ebeid, in *Deep Centers in Semiconductors*, edited by S.T. Pantelides (Gordon and Breach, New York, 1986).
- ⁶H.Ch. Alt, *Appl. Phys. Lett.* **54**, 1445 (1989); **55**, 2736 (1989); *Phys. Rev. Lett.* **65**, 3421 (1990).
- ⁷C. Song, B. Pajot, and F. Gendron, *J. Appl. Phys.* **67**, 7307 (1990).
- ⁸M. Linde, J.-M. Spaeth, and H.Ch. Alt, *Appl. Phys. Lett.* **67**, 662 (1995).
- ⁹G.D. Watkins, and J.W. Corbett, *Phys. Rev.* **121**, 1001 (1961).
- ¹⁰W. Kohn and L.J. Sham, *Phys. Rev.* **140**, A1133 (1965).
- ¹¹R. Jones, and S. Öberg, *Phys. Rev. Lett.* **69**, 136 (1992).
- ¹²T. Mattila and R.M. Nieminen, *Phys. Rev. B* **54**, 16 676 (1996).
- ¹³A. Taguchi and H. Kageshima, *Phys. Rev. B* **57**, R6779 (1998).
- ¹⁴M. Pesola, J. von Boehm, T. Mattila, and R.M. Nieminen, *Phys. Rev. B* **60**, 11 449 (1999).
- ¹⁵S. Pöykkö, M.J. Puska, and R.M. Nieminen, *Phys. Rev. B* **57**, 12 174 (1998).
- ¹⁶D. Vanderbilt, *Phys. Rev. B* **41**, 7892 (1990); K. Laasonen, A. Pasquarello, R. Car, C. Lee, and D. Vanderbilt, *ibid.* **47**, 10 142 (1993).
- ¹⁷D.R. Hamann, *Phys. Rev. B* **40**, 2980 (1989).
- ¹⁸S.G. Louie, S. Froyen, and M.L. Cohen, *Phys. Rev. B* **26**, 1738 (1982).
- ¹⁹H.J. Monkhorst and J.D. Pack, *Phys. Rev. B* **13**, 5188 (1976).
- ²⁰The kinetic energy cut-off change from 25 Ry to 30 Ry when using 2^3 Monkhorst-Pack (MP) \mathbf{k} points, and a 32 atom-site supercell including one O atom, shifts the energy/atom by 0.04 eV downwards. A bulk calculation using 2^3 MP \mathbf{k} points (Γ point) and a 32 atom-site (128 atom-site) supercell, results in energy/atom which lies 0.002 (0.096) eV above that resulting from an accurate calculation using 6^3 MP \mathbf{k} points and a 2 atom-site primitive unit cell.
- ²¹S. Pöykkö, M.J. Puska, and R.M. Nieminen, *Phys. Rev. B* **53**, 3813 (1996).
- ²²Th. Köhler, Th. Frauenheim, and G. Jungnickel, *Phys. Rev. B* **52**, 11 837 (1995).
- ²³M. Skowronski, S.T. Neild, and R.E. Kremer, *Appl. Phys. Lett.* **57**, 902 (1990).
- ²⁴C. Song, B. Pajot, and C. Porte, *Phys. Rev. B* **41**, 12 330 (1990).
- ²⁵G.A. Samara, M. Skowronski, and W.C. Mitchel, *J. Phys. Chem. Solids* **56**, 625 (1995).
- ²⁶J.F. Janak, *Phys. Rev. B* **18**, 7165 (1978).
- ²⁷H.J. von Bardeleben, J.C. Bourgoin, and A. Miret, *Phys. Rev. B* **34**, 1360 (1986).
- ²⁸S. Pöykkö, M.J. Puska, M. Alatalo, and R.M. Nieminen, *Phys. Rev. B* **54**, 7909 (1996).